MATERIALS PHYSICS AND MECHANICS RESEARCH ARTICLE

Submitted: July 14, 2025 **Revised: October 29, 2025** **Accepted: December 19, 2025**

Comprehensive study on PbO–MO (M=Mg, Zn, Cd)–As_2O_3:Tm_2O_3 glasses physical and optical properties

P.R. Rao [1], P. Naresh [2], N.N. Rao [1]✉, B.J.R.S.N. Swamy [1], A.C. Babu [3], N.Ch.R. Babu [4]

[1] Krishna University Dr. MRAR College of PG Studies, Nuzvid, India

[2] Velagapudi Ramakrishna Siddhartha School of Engineering, Siddhartha Academy of Higher Education (SAHE) Deemed to be University, Vijayawada, India

[3] Sir C. R. Reddy College of Engineering, Eluru, India

[4] Rajiv Gandhi University of Knowledge Technologies (AP-IIIT), Nuzvid, India

✉ nnrphy@gmail.com

ABSTRACT

Three modifier oxides, MgO, ZnO, and CdO, were mixed with 1.0 mol % of Thulium-doped lead arsenate glasses and were synthesized by the usage of melt-quenching technique. XRD patterns clearly show the evidence that samples are amorphous and had been supported with the aid of using the lack of distinct peaks. Various functional physical parameters such as molar volume, oxygen packing density (OPD), Tm^{3+} ion concentration, mean Tm^{3+} ion separation, polaron radius are evaluated by using experimentally measured densities and refractive indices. The optical absorption spectra of PbO–MO (M = Mg, Zn, Cd)–As_2O_3:Tm_2O_3 glass system have been studied. Through the application of least square fitting analysis, the J-O phenomenological parameters (Ω_2, Ω_4, Ω_6) for the three glass systems have been calculated.

KEYWORDS

optical absorption • XRD • As_2O_3 glasses • JO parameters • rare earth doped glasses

Citation: Rao PR, Naresh P, Rao NN, Swamy BJRSN, Babu AC, Babu NChR. Comprehensive study on PbO–MO (M=Mg, Zn, Cd)–As_2O_3:Tm_2O_3 glasses physical and optical properties. *Materials Physics and Mechanics*. 2026;54(1): 24–33. http://dx.doi.org/10.18149/MPM.5412026_4

Introduction

In the glass system, rare-earth ions have been thoroughly studied with respect to both their physical and chemical characteristics inside the network of glasses, which establishes the glass structure, it also incorporates optical characteristics [1,2]. Because of its exceptional prospective applications, the developments of glasses which are doped with rare-earth ions are precisely on course because of their use, including optical, semiconductors, sensors, lasers, etc. [3,4].The composition, structure and qualities of the final glass materials are directly influenced by the production technology and chemical and mineralogical makeup of the raw materials [5].

However, lead arsenic glasses are highly toxic, volatile easily at high temperature and chemical instable in moisture due to their devitrification, surface leaching along with hydrolytic attack. From the literature study [6–8], it strongly evidence that, the incorporation of suitable network modifiers/intermediate modifier like CuO, WO_3, Fe_2O_3, etc., there is change to reduce the number of non-bridging oxygens (NBOs) by forming more stable M–O–As (M = metal) linkages significantly improved the chemical durability, reducing moisture induced surface leaching and enhances long-term stability. Furthermore, the

presence of these oxides minimizes structural defects, enhances homogeneity, which leads the tuning of physical parameters such as density, refractive index and optical band gap. Tuning effect of the modifiers for getting stable and modified $PbO-As_2O_3$ glasses not only governed by the chemical composition nature but also their relative proportion in the glass matrix. Thus, the strategic addition of MgO/ZnO/CdO effectively mitigates the weaknesses of $PbO-As_2O_3$ glasses and enables the development of compositionally stable materials for advanced optical and photonic applications and also it nevertheless to mention that no literature available with systematic replacement of divalent modifier in the $PbO-As_2O_3$ glass host.

The RE^{3+} (Ln^{3+}) ions doped glasses are highly renowned because of their high efficient optical property and good transparency in near and mid IR region [9]. Thulium (Tm^{3+}) is recognized as one of the most potent active ions [10]. Recently, considerable attention has been given to analyzing the spectra of Tm^{3+} ions in various glass hosts, since this ion exhibits emission in the infrared region (~ 2 μm), making the glasses suitable for eye-safe LIDAR [11], gas sensors, pollution monitoring in atmosphere, biomolecule sensors, laser guided military applications etc., [12,13]. Because of the possibility of up – conversion from infrared to visible light, these ions are well-known [14–16].

Among Oxide glasses, $PbO-As_2O_3$ glasses exhibit high density and good optical transparency, which are essential for optimum efficiency for optical pumping. Metal oxides have been shown to improve the optical properties of glass, making them promising material for optical fiber amplifiers, non-linear optical systems, electronic optical switches etc. [17]. When lead arsenates glasses are modified with network altering metal ions, structural changes and local field fluctuations can be expected; these modifications may significantly influence the optical transitions of lanthanide ions and enhances the compositional stability. In this ongoing work, we report the physical, optical studies and their correlation in $PbO–MgO/ZnO/CdO–As_2O_3$ glasses doped with Tm^{3+} ions.

Materials and Methods

The present studied glass samples had been prepared by adopting the melting and quenching method. Within the area where glass is formed, the compositions selected for the current investigation is $20PbO-5MO$ (M = Mg, Zn, Cd)$-74As_2O_3{:}1.0Tm_2O_3$ all in mol % weighted by using Essce Vibra HT digital weighting balance with maximum capacity 100 gm and readability 0.1 mg. Figure 1 depicts a flow chart of the glass sample preparation process. The specific chemical composition and their codes used for present prepared samples were displayed in Table 1. All compositions were melted in platinum crucibles at 700 °C using muffle furnace. The melts were then rapidly quenched by pouring onto a preheated brass mould to avoid crystallization. The obtained glass samples were subsequently annealed at 250 °C for three hours at a cooling rate of 1 °C/min to relieve internal stresses and ensure structural stability. Figure 2 shows

Table 1. Composition of glass samples (all in mol %)

Sample Code	PbO	MO	As_2O_3	Tm_2O_3
GM	20	5.0 MgO	74	1.0
GZ	20	5.0 ZnO	74	1.0
GC	20	5.0 CdO	74	1.0

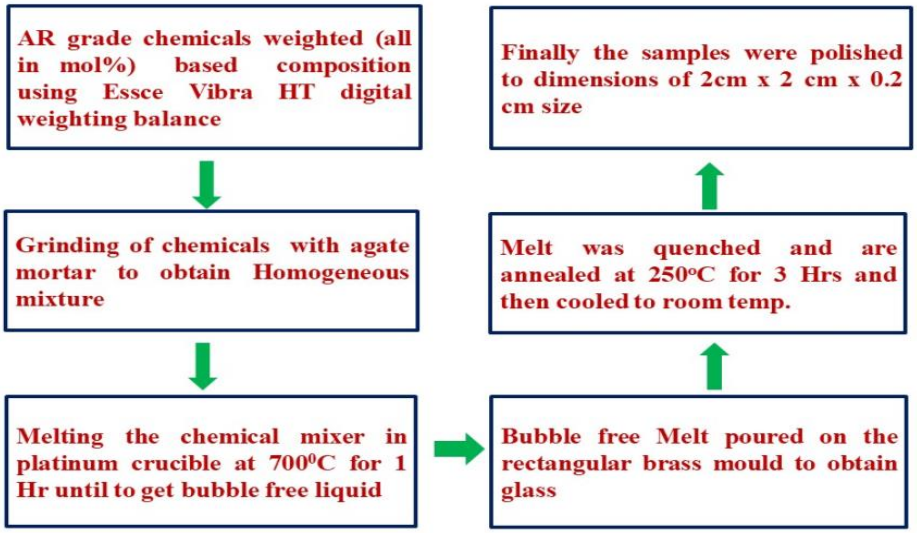

Fig. 1. Flow chart of various steps involved in PbO–MO (MgO/ZnO/CdO)–As_2O_3:Tm_2O_3 glass samples

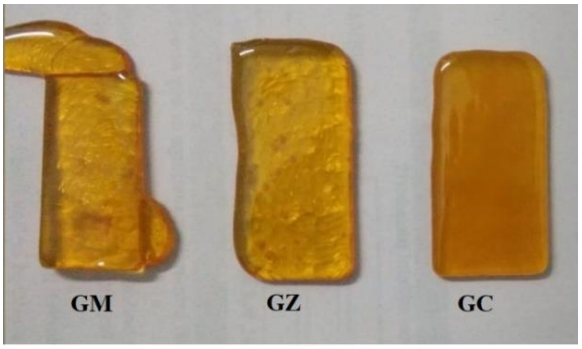

Fig.2. Photograph of prepared PbO–MO (MgO/ ZnO/CdO)–As_2O_3:Tm_2O_3 glass samples

the digital photographs of the prepared PbO–MO (M = Mg, Zn, Cd)–As_2O_3:Tm_2O_3 glasses, which clearly exhibits that the prepared samples are light yellow in colour with good transparency, and absence of visible surface defects, confirming the good quality of the synthesized glasses. Density determination was done by adopting Archimedes' principle by measuring the weights of the prepared samples in air as well in acetone by using Essce Vibra HT digital weighting balance. The refractive index of the samples was measured by using Abbe refractometer using Abbe refractometer (Model NAR-4T: Resolution ± 0.001 nD and accuracy ± 0.0002 nD) with mono bromo naphthalene as the contact layer between the glass and the refractometer prism. The amorphous nature of the prepared glasses was checked by X-ray diffraction spectra recorded on Rigaku D/Max ULTIMA III X-ray diffractometer with CuK_α (λ = 0.15406 nm) radiation. The optical absorption spectra of the glasses at ambient temperature were recorded using JASCO Model V-970 UV- vis-NIR spectrophotometer with spectral resolution of 0.1 nm.

Results and Discussion

The density of the samples was calculated using Archimedes' standard principle by measuring their weights in air (W_a) as well as in acetone (W_l) as a buoyant liquid. With the help of measured density, estimated average molecular weight of the individual samples,

several important characteristic physical parameters, including molar volume, oxygen packing density (OPD), Tm^{3+} ion concentration, mean Tm^{3+} ion separation, polaron radius were calculated from standard relation and presented in Table 2 [18,19]. From the obtained and presented data from Table 2, it was noticed pragmatically among samples containing MgO, ZnO and CdO, that density is larger for GC, large for GZ and small for GM samples. In contrast molar volume shows as usual inverse behavior with densities of the glass samples. This was unexpected trend why because due to the replacement of the Mg^{2+} ions with higher molecular mass (ionic radius) ions like Zn^{2+} and Cd^{2+} we expect the reverse trend, which suggests that evidently takes place structural changes in the glass matrix. Among the present reported samples, OPD is smaller for GM, small for GZ and larger for GC. This increase in OPD suggests that the glass structure becomes compact hence leads to increase the density of the glass samples.

Table 2. Physical parameters of PbO–MO (M = Mg, Zn, Cd)–As_2O_3:Tm_2O_3 glasses

Property	Standard relation	Sample code		
		GM	GZ	GC
Average molecular weight ($\bar{M}$), g/mol	$\bar{M} = \sum X_i M_i$	197.52	199.17	201.05
Density (ρ), g/cm^3	$\rho = \left(\frac{W_a}{W_a - W_l}\right)\rho_b$	5.174	5.382	5.540
Molar volume (V_m), cm^3/mol	$V_m = \frac{\bar{M}}{\rho}$	38.176	37.006	36.290
Oxygen packing density (OPD), atoms/cm^3	$OPD = n\left(\frac{\rho}{\bar{M}}\right)1000$	63.13	65.12	66.41
Refractive index (n)	Experimental value	1.654	1.655	1.656
Molar refractivity (R_m), cm^3/mol	$R_m = \left(\frac{n^2-1}{n^2+2}\right)V_m$	13.99	13.58	13.33
Molar electronic polarizability (α_m), cm^3/mol	$\alpha_m = \frac{R_m}{2.52}$	5.552	5.389	5.291
Electronic polarizability (α_e), 10^{-25} cm^3	$\alpha_e = \frac{3(n^2-1)}{4\pi N_A(n^2+2)}$	1.454	1.455	1.457
Metallization criterion (M)	$M = 1 - \frac{R_m}{V_m}$	0.6335	0.6330	0.6326
Optical basicity (Λ)	$\Lambda = \sum x_i \Lambda_i$	1.037	1.044	1.050
Tm^{3+} ion concentration N_i, 10^{24} ions/cm^3	$N_i = \frac{N_A x_i \rho}{\bar{M}}$	1.577	1.627	1.659
Interionic distance (r_i), Å	$r_i = \left[\frac{1}{N_i}\right]^{\frac{1}{3}}$	8.590	8.502	8.447
Polaron radius r_p, Å	$r_p = \frac{1}{2}\left[\frac{\pi}{6N_i}\right]^{\frac{1}{3}}$	3.461	3.426	3.403
Field strength (F_i), 10^{15} cm^{-2}	$F_i = \frac{Z}{r_p^2}$	1.379	1.301	1.380

The refractive index (n) values were measured using monochromatic LED light of a wavelength 589.3 nm. The refractive index values for the studied samples were closely 1.65 to 1.66 following the trend $n_{GM} < n_{GZ} < n_{GC}$. Using standard relations along with the measured refractive indices, the physical parameters such as molar refractivity, molar electronic polarizability, metallization criteria and optical basicity were evaluated and the same were systematically presented in Table 2, where X_i is the mol % of the oxide

compound,M_i is the molecular weight of the oxide compound, ρ_b is the density of acetone, N_A is the Avogadro number, Λ_i is the specific basicity moderating parameter of ith oxide compound, Z is the thickness of the sample.

Figure 3 depicts the observed XRD patterns of the GM, GZ and GC samples. These patterns exhibit no sharp peak, confirming the amorphous nature of the prepared samples. Instead, two broad diffuse maxima are observed centered near $2\theta \approx 30°$ and $\approx 50°$. In amorphous materials such as oxide glasses, these broad halos arise by diffuse scattering that originates from short range and medium range atomic correlations, rather than from long range periodicity. The high angle halo near $\approx 50°$ arises from short range order corresponding to the nearest neighbour cation oxygen bond distances ($d \approx 1.8$ Å) with in the basic structural units present in the glass formers such as SiO_4 tetrahedral, BO_3/BO_4 units, AsO_3 pyramids, Pb-O polyhedra and modifier oxygen linkages [20,21]. Whereas the low angle halo near $\approx 30°$ arises from medium range order especially in oxide glasses corresponding due to the long-range real spaces distances between inter polyhedral correlations like AsO_3 units PbO ($d \approx 3$ Å). In addition, the presence of MgO, ZnO, and CdO modifiers enhances such medium-range structural organization due to variations in bonding strength, cation size, and field strength, thereby making the ~ 30° halo more prominent.

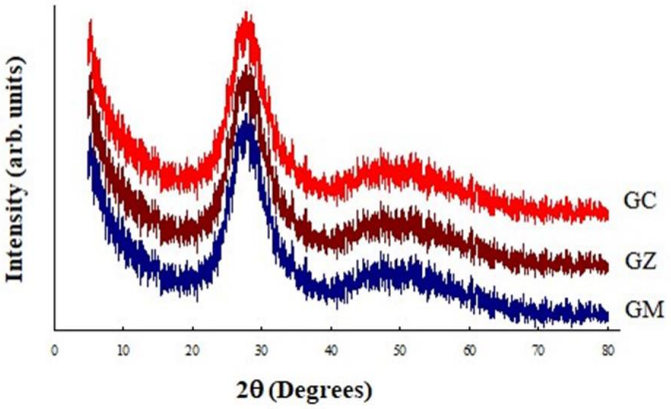

Fig. 3. X-ray diffraction pattern for PbO–MO (M=Mg, Zn,Cd) As_2O_3:Tm_2O_3 glasses

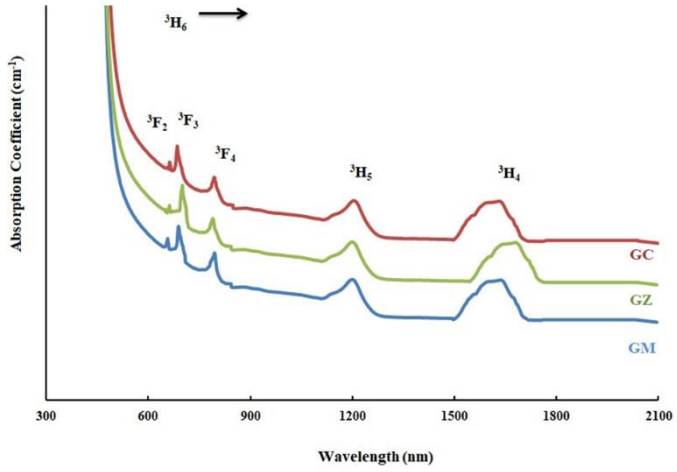

Fig.4. Optical absorption spectra of PbO–MO (M=Mg, Zn, Cd)–As_2O_3 glasses doped with Tm_2O_3

The optical absorption spectra of GM, GZ and GC glass samples within the wavelength range of 300–2100 nm were presented in Figure 4. Glass sample GM exhibits five distinct absorption peaks with peak positions at about 657, 689, 795, 1199, 1631 nm; among them, first one with less intensity appeared as a kink, whereas last one was a boarder. These identified peaks were attributed due to the transition Tm^{3+} ions from the ground state $^3H_6$ to the higher energy states $^3F_2$, $^3F_3$, $^3F_4$, $^3H_5$, $^3H_4$ respectively [22,23]. Among the three prepared samples, the other two samples also exhibit similar absorption bands with marginal blue shift in wavelengths, the corresponding energies of these transitions are presented in Table 3.

Table 3. The absorption band energies (cm^{-1}), the experimental (f_{exp}) and calculated (f_{cal}) oscillator strengths for the absorption transitions of PbO–MO (M = Mg, Zn, Cd)–As_2O_3:Tm_2O_3 glasses

Transitions	GM				GZ				GC			
	Energy ν, cm^{-1}	f_{exp}, 10^{-6}	f_{cal}, 10^{-6}	% diff	Energy ν, cm^{-1}	f_{exp}, 10^{-6}	f_{cal}, 10^{-6}	% diff	Energy ν, cm^{-1}	f_{exp}, 10^{-6}	f_{cal}, 10^{-6}	% diff
$^3H_6 \rightarrow {}^3F_2$	15231	2.08	2.1	0.96	15104	1.16	1.15	0.86	15092	2.89	2.35	18.68
$\rightarrow {}^3F_3$	14510	6.34	6.7	5.67	14280	5.71	6.30	10.33	14596	6.60	5.94	10.00
$\rightarrow {}^3F_4$	12584	3.92	4.08	4.08	12608	3.47	3.70	6.62	12610	3.48	3.60	3.49
$\rightarrow {}^3H_5$	8338	4.57	4.82	5.47	8314	4.51	4.63	2.66	8320	4.69	4.80	2.34
$\rightarrow {}^3H_4$	6130	3.50	3.61	3.14	5960	2.48	2.57	2.01	6131	3.72	3.68	1.08
Direct band gap, eV	2.49				2.52				2.55			
Indirect band gap, eV	2.59				2.61				2.62			
R.m.s. % deviation	4.23				5.70				9.67			

Judd-Ofelt (J–O) parameters are vital to enhancing the comprehension of optical characteristics, particularly concerning rare-earth ions such as thulium in glass matrices. They bid valuable insights into properties like, radiative transition probabilities, oscillator strengths, and branching ratios etc.

By applying J–O theory and measuring the area under the absorption curves, the experimental oscillator strengths were determined by the simplified relation [24]:

$$f_{exp} = 4.318\ X\ 10^{-9} \int \varepsilon(\vartheta)\, d\vartheta, \quad (1)$$

where $\int \varepsilon(\vartheta)\, d\vartheta$ is the area under the absorption curve, $\varepsilon(\vartheta)$ is the molar absorptivity of the respective band at ϑ:

$$\varepsilon(\vartheta) = \frac{A}{cl}, \quad (2)$$

where $\frac{A}{l}$ is the absorbance coefficient, c is the concentration of the lanthanide ion.

The calculated oscillator strengths for the electric dipole transition from the ground state (ψ) to the excited state (ψ') were obtained using the relation:

$$f_{cal} = \left(\frac{8\pi^2 mcv}{3h(2J+1)}\right)\left(\frac{(n^2+2)^2}{9n}\right)\sum_{\lambda=2,4,6} \Omega_\lambda \left(\langle \psi_{J'} \rangle\right)^2, \quad (3)$$

where all the terms having their own standard meaning, which are mentioned in the literature [22,24], $\|U^\lambda\|$ are the square reduced matrix element of the unit tensor operator of the rank $\lambda = 2, 4, 6$, these standard values were acquired from [25]. The root mean square deviation values from the calculated and experimental oscillator strengths were

obtained using the basic relation, which helps to understand the fitment of theoretical data with experimental data in the RE-doped glasses:

$$\text{RMS } \% = 100 \sum \frac{(f_{cal} - f_{exp})^2}{N}. \quad (4)$$

The absorption band energies (cm^{-1}), the experimental (f_{exp}) and calculated (f_{cal}) oscillator strengths calculated for the absorption band intensities of PbO–MO (M = Mg, Zn, Cd)–As_2O_3:Tm_2O_3 glasses were presented as Table 3.

Using least squares fitting analysis, J–O parameters T_λ $(\lambda = 2,4,6)$ were determined with help of values $\|U^\lambda\|^2$(taken form the literature ref), f_{exp}, f_{cal}, and v by the relation [26]:

$$f_c = [T_2(\|U^2\|)^2 + T_4(\|U^4\|)^2 + T_6(\|U^6\|)^2]\vartheta. \quad (5)$$

J–O Intensity parameters $\Omega_\lambda(\lambda = 2,4,6)$ are calculated from above obtained $T_\lambda(\lambda = 2,4,6)$ using the equation:

$$\Omega_\lambda = \left(\frac{3h}{8\pi^2 mc}\right)\left(\frac{9n}{(n^2+2)^2}\right)(2J+1)T_\lambda, \quad (6)$$

where all symbols have their own significant meaning as mentioned in literature [25,26], J is taken as 13 for the ground state of Tm^{3+} ion. The obtained J–O intensity parameters $\Omega_\lambda(\lambda = 2,4,6)$ for Tm_2O_3 doped PbO–MO (M = Mg, Zn, Cd)–As_2O_3 glasses are displayed in Table 4. When the computed oscillator strengths are compared to the experimental oscillator strengths, a fair match is made. The root mean square percentage (RMS %) deviation between f_{exp} and f_{calc} is used to express the fit quality. The J–O theory's validity and suitability for the current glasses are confirmed by the comparatively low levels of these deviations [27]. In complex hosts like glass it is common that individual transition oscillator strengths differ by 10–30 % from calculated values; an RMS percentage deviation (RMS %) below ~ 20–30 % is usually considered acceptable as indicating a good correlation in rare-earth–doped glasses. For the present studied three samples, RMS % deviation is observed < 10 which represents the overall "goodness of fit" and validates whether the derived J–O parameters Ω_2, Ω_4, Ω_6 are reliable.

Table 4. J–O parameters (Ω_λ) and the bonding parameter (δ') of PbO–MO (M=Mg, Zn, Cd)–As_2O_3:Tm_2O_3 glasses and their comparison with the previous work of different glasses

Glass	Ω_2, 10^{-20} cm^2	Ω_4, 10^{-20} cm^2	Ω_6, 10^{-20} cm^2	Ω_4/Ω_6	δ'	Ref.
GM	8.35	0.863	0.336	2.56	-0.160	Present work
GZ	7.81	0.810	0.370	2.18	-0.948	Present work
GC	6.74	0.780	0.362	2.15	-1.050	Present work
PSBT	3.66	2.926	1.549	1.89	---	[22]
BBT	3.65	1.32	1.37	0.96	---	[23]
Glass B	4.15	0.80	0.40	2.00	---	[24]
Gallate	4.79	1.52	0.58	2.62	---	[28]
Germanate	4.10	0.99	0.26	3.80	---	
Aluminate	4.94	1.67	0.61	2.73	---	

Hence, the Ω_2 parameter acts like a strain for the asymmetry of the ligand field, reflecting the degree to which the local symmetry is distorted. For all the present three sets of glasses, the values of Ω_λ are projected primarily in the following sequence; $\Omega_2 > \Omega_4 > \Omega_6$ [28]. Further, it is identified that this phenomenological intensity parameter Ω_λ for λ = 2, 4 observed lower when Mg was replaced by the Zn and Cd, whereas for λ = 6, it is observed to rise with the replacement of Zn and Cd by the Mg in the glass matrices.

These results reflect among the three studied present glasses: GM has more covalent behavior than the other two. Afterward coming to the Ω_4, bids attention to the interaction of RE-ions with the atom that are away in the lattice i.e., tells about medium-range interactions that reflects the rigidity and bulk properties like density, mechanical strength and elasticity etc., Approaching to the third one, Ω_6 reveals the information about long-range interactions between the RE-ion and its environment, which plays an active role on optical and efficiency, non-radiative transitions, phonon interaction (Luminescence efficiency). Lower Ω_6 values claim less rigid, faster non- radiative relaxations due to interaction of RE-ions with lattice by producing lattice vibrations (phonons). Hence, by the obtained results, it may except that GM glass samples were rigid with lower non-radiative relaxations, same result was confirmed the higher Ω_4/Ω_6 value.

The bonding parameter (δ) which also helps to estimate the covalent character of the RE ions with the ligand bond has been calculated for each of the three glasses using the equation:

$$\delta = \frac{\Omega_2 - \Omega_2^{free-ion}}{\Omega_2^{free-ion}}. \quad (7)$$

The RE-ion Tm^{3+} in MgO mixed glass has the highest δ value, whereas CdO mixed glass exhibits the lowest δ value. The bonding parameter value might potentially be used as additional evidence for this claim. Hence, Optical data with the fitment of J–O theory imply that the Tm^{3+} environment in MgO glasses is a more covalent character with a rigid structure having higher luminescence efficiency than the other two glasses containing ZnO and CdO.

According to Davis and Mott's theory [29,30], the optical edge of non-crystallize materials can be expressed by the equation:

$$\alpha h\vartheta = A\left(h\vartheta - E_{opt}\right)^r, \quad (8)$$

where α is the absorption coefficient, A is the proportionality constant, $h\nu$ is photon energy, E_{opt} is the optical band gap energy, r = 2(allowed indirect), ½ (allowed direct) – transitions respectively. The direct and indirect optical band gaps were estimated by extrapolations of the $(\alpha h\vartheta)^r vs\ h\vartheta$ curves at $(\alpha h\vartheta)^r = 0$.

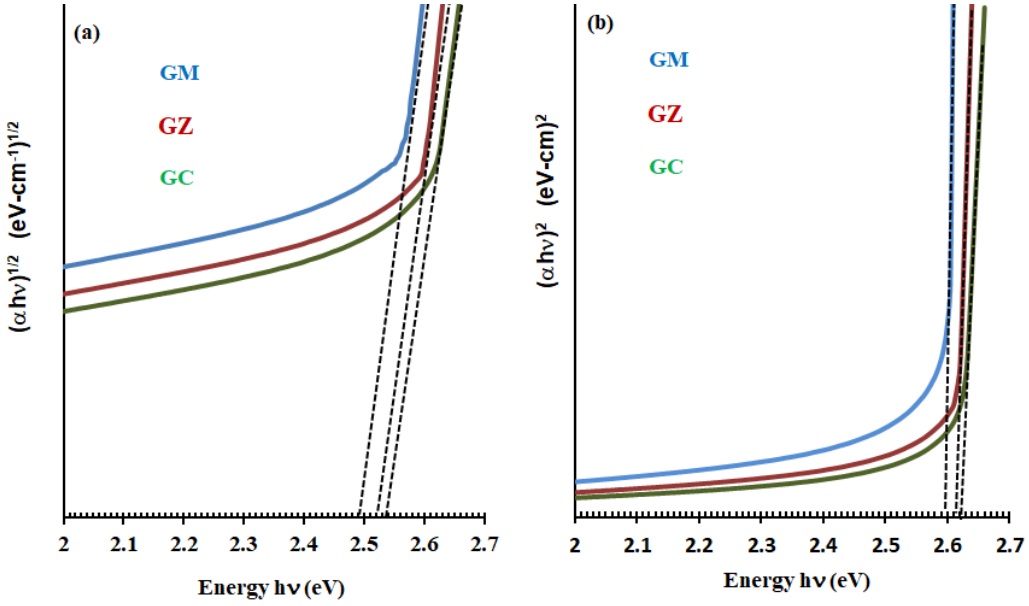

Fig. 5. Urbach plots of PbO–MO (M=Mg, Zn, Cd)–As_2O_3 glasses doped with Tm_2O_3: (a) direct; (b) indirect

Figure 5 shows $(\alpha h\vartheta)^r vs\ h\vartheta$ plots of PbO–MO–As_2O_3:Tm_2O_3 glasses. From the extrapolations, the GM glass exhibits optical direct and indirect band gaps of approximately 2.54 and 2.75 eV. Replacing ZnO or CdO with MgO produces a small but systematic increase (widening) of both direct and indirect band gaps (Table 4), reflecting reduced modified local structure from Mg^{2+} incorporation. In other way, ZnO and CdO introduce highly polarizable cations, which increase the electron donating ability of O^{2-} and cause to produce more NBOs. This increases optical basicity and raised the J–O parameter Ω_2 supports the same with causes the reduced covalency and local structural distortion around Tm^{3+} ions, leading to a more rigid matrix and higher energy optical transitions.

Conclusions

An assortment of glass systems with chemical substance 20 PbO–5 MO (M = Mg, Zn, Cd)–74 As_2O_3:1.0Tm_2O_3 was successfully prepared by conventional melt-quenching technique. The density and molar volume of the glass were found to change when MO was added to the glass system. The transitions below have been identified by glasses optical absorption spectrum $^3H_6 \rightarrow {}^3F_2$, $^3F_3$, $^3F_4$, $^3H_5$, $^3H_4$. The optical absorption spectra of these ions may be described using the J–O theory for each of the three glass systems. The J–O parameters for the three systems are calculated using least squares fitting analysis and the results indicate the following pattern: $\Omega_2 > \Omega_4 > \Omega_6$. The glasses that were combined with magnesium oxide had the highest bonding parameter *δ,* smaller optical band gaps all the above observations clearly indicate that the rare earth ions in this glass matrix have a larger covalent environment in glass containing MgO.

CRediT authorship contribution statement

Paritala R. Rao: investigation; **Padamati Naresh**: formal analysis, writing – original draft; **Narasimha N. Rao**: writing – review & editing; **Bhogi Jai Rama Satyanarayana N. Swamy**: conceptualization; **A. Chitti Babu**: validation & review; **N.Ch. Ramesh Babu**: investigation.

Conflict of interest

The authors declare that they have no conflict of interest.

References

1. Azman K, Azhan H, Syamsyir SYS, Mardhiah A, Nasuha MRS. Optical properties of Nd doped lead borotellurite glass. *Materials Science Forum.* 2016;846: 193–198.
2. Malge A, Sankarappa T, Sujatha T, Abdul Azeem P, Devidas GB, Kori S. Structural and DC conductivity studies of borotellurite glasses doped with ZnO, Li_2O and Dy_2O_3. *Materials Today: Proceedings.* 2020;26(2): 1960–1963.
3. Shirshnev PS, Snezhnaia ZG, Shirshneva-Vaschenko EV, Romanov AE, Bougrov VE. Relation of the optical properties of boron copper-containing glasses on the concentration of lithium. *Materials Physics and Mechanics.* 2018;40(1): 78–83.
4. Klinkov V, Archelkov VB, Semencha AV, Tsimerman EA, Sedegova TY, Rudskoy AI. Halide-containing zinc borosilicate glass as a matrix for $CsPbBr_3$ crystal. *Materials Physics and Mechanics.* 2023;51(2): 27–35.
5. Rodin AI, Ermakov AA, Erofeeva IV, Erofeev VT. Structure and properties of porous glass ceramics from siliceous rocks with the addition of $Mg(OH)_2$. *Materials Physics and Mechanics.* 2023;51(5): 127–141.

6. Kalyani B, Pujari N, Edukondalu A, Reddy MS, Vardhani CP. AC Conductivity and dielectric relaxation in $Li_2O-PbO-As_2O_3-B_2O_3$ glasses. *Chinese Journal of Physics.* 2022;79: 141–150.
7. Satyanarayana T, Nagarjuna G, Kiran KR. Spectral features of lead arsenate glasses doped with copper oxide. *Solid State Phenomena.* 2013;207: 55–67.
8. Srinivasarao G, Veeraiah N. The effect of tungsten ions on the structure of $PbO-As_2O_3$ glasses. *Physica Status Solidi A.* 2002;191(2): 370–386.
9. Jackson SD. Cross relaxation and energy transfer upconversion processes relevant to the functioning of 2 μm Tm^{3+}-doped silica fibre lasers. *Optics Communications.* 2004;230(1–3): 197–203.
10. Gebavi H, Milanese D, Liao G, Chen Q, Ferraris M, Ivanda M, Gamulin O, Taccheo S. Spectroscopic investigation and optical characterization of novel highly thulium doped tellurite glasses. *Journal of Non-Crystalline Solids.* 2009;355(9): 548–555.
11. Lakshminarayana G, Meza-Rocha AN, Soriano-Romeo O, Huerta EF, Caldiño U, Lira A, Lee D-E, Yoon J, Park T. Survey of optical and fluorescence traits of Tm^{3+}-doped alkali/mixed alkali oxides constituting $B_2O_3-BaO-ZnO-LiF$ glasses for 0.45 μm laser and 1.46 μm fiber amplifier. *Results in Physics.* 2021;26: 104343.
12. Peng B, Izumitani T. Optical properties, fluorescence mechanisms and energy transfer in Tm^{3+}, Ho^{3+} and $Tm^{3+}-Ho^{3+}$ doped near-infrared laser glasses sensitized by Yb^{3+}. *Optical Materials.* 1995;4(6): 797–810.
13. Song X, Han K, Zhou D, Xu P, Zhang P. Broadband ~1.8 μm emission characteristics of Tm^{3+}-doped bismuth germanate glass based on Ga_2O_3 modification. *Journal of Non-Crystalline Solids.* 2021;557: 120575.
14. Tanabe S, Hanada T. Effect of ligand field on branching ratio of ultraviolet and blue upconversions of Tm^{3+} ions in halide and oxide glasses. *Journal of Applied Physics.* 1994;76(6): 3730–3734.
15. Hirao K, Tamai K, Tanabe S, Soga N. Frequency upconversion and its new mechanism in Tm^{3+}-doped fluoroaluminate glasses. *Journal of Non-Crystalline Solids.* 1993;160(3): 261–267.
16. Otto AP, Brewer KS, Silversmith AJ. Red to blue upconversion in Tm-doped sol–gel silicate glasses. *Journal of Non-Crystalline Solids.* 2000;265(1–2): 176–180.
17. Muhammad Noorazlan A, Mohamed Kamari H, Zulkefly SS, Mohamad DW. Effect of erbium nanoparticles on optical properties of zinc borotellurite glass system. *Journal of Nanomaterials.* 2013;2013(1): 940917.
18. Rao NN, Naresh P, Rao PR, Swamy BJRSN, Babu AC. Influence of modifier oxide on spectroscopic features of $ZnO-CaF_2-CuO-B_2O_3:R_2O$ glasses (R = Li, Na & K). *AIP Conference Proceedings.* 2023;2368(1): 020005.
19. Biradar S, Dinkar A, Manjunatha, Bennal AS, Devidas GB, Hareesh BT, Siri MK, Nandan KN, Sayyed MI, Es-soufi H, Chandrashekara MN. Comprehensive investigation of borate-based glasses doped with BaO: An assessment of physical, structural, thermal, optical, and radiation shielding properties. *Optical Materials.* 2024;150: 115176.
20. Li J, Sun Y, Li Z, Zhang Z. Short-range and medium-range structural order in $CaO-SiO_2-TiO_2-B_2O_3$ glasses. *ISIJ International.* 2016;56(5): 752–758.
21. N'Dri K, Houphouet-Boigny D, Jumas J-C. Study of first sharp diffraction peak in As_2O_3 glasses by X-ray powder diffraction method. *Journal of Non-Oxide Glasses.* 2012;4(3): 29–37.
22. Satyanarayana T, Kityk IV, Brik MG, Ravi Kumar V, Veeraiah N. Fluorescence features of Tm^{3+} ions in $PbO-Sb_2O_3-B_2O_3$ glass ceramics. *Physica B: Condensed Matter.* 2010;405(7): 1872–1880.
23. Xu Z, Chen Y, Lin Y, Gong X, Luo Z, Huang Y. Effect of concentration on the spectral properties of Tm^{3+} ions in bismuth borate glasses. *Journal of Alloys and Compounds.* 2009;481(1–2): 411–416.
24. Ratnakaram YC, Thirupathi Naidu D, Vijaya Kumar A, Rao JL. Characterization of Tm^{3+} doped mixed alkali borate glasses—spectroscopic investigations. *Journal of Physics and Chemistry of Solids.* 2003;64(12): 2487–2495.
25. Carnall W, Crosswhite H, Crosswhite HM. *Energy level structure and transition probabilities in the spectra of the trivalent lanthanides in LaF_3.* Argonne (IL): Argonne National Laboratory; 1978.
26. Lakshman SVJ, Ratnakaram YC. Spectral studies of praseodymium(III) and thulium(III) in certain sulphate glasses. *Journal of the Less Common Metals.* 1986;126: 227–232.
27. Zhang Y, Liu J-M, Liu M-H, Zhang Z-B, Wong W-H, Zhang D-L. Error evaluation of Judd–Ofelt spectroscopic analysis. *Spectrochimica Acta Part A: Molecular and Biomolecular Spectroscopy.* 2020;239: 118536.
28. Zou X, Izumitani T. Fluorescence mechanisms and dynamics of Tm^{3+} singly doped and Yb^{3+}, Tm^{3+} doubly doped glasses. *Journal of Non-Crystalline Solids.* 1993;162(1–2): 58–67.
29. Davis EA, Mott NF. Conduction in non-crystalline systems V. Conductivity, optical absorption and photoconductivity in amorphous semiconductors. *Philosophical Magazine.* 1970;22(179): 903–922.
30. Tauc J. (Ed.) *Amorphous and liquid semiconductors.* Berlin: Springer; 2012.